

Isospin dependence of pion absorption by nucleon pairs  
in the He isotopes

H. Toki and H. Sarafian

National Superconducting Cyclotron Laboratory  
and Department of Physics-Astronomy  
Michigan State University  
East Lansing, Michigan 48824-1321

ABSTRACT

We calculate the relative absorption ratio of a pion by  $T=0$  and  $T=1$  nucleon pairs in the He isotopes measured recently by Ashery, et al. Standard theory based on  $\Delta$ -isobar intermediate excitations agrees with the experimental observation that for energies around the resonance, pion absorption by a  $T=1$  nucleon pair is strongly suppressed.

Very recently Ashery et al.<sup>1</sup> performed the  $(\pi^+, 2p)$  and  $(\pi^-, pn)$  measurements on  ${}^3\text{He}$  and  ${}^4\text{He}$  at pion kinetic energy of  $T_\pi = 165$  MeV in order to obtain information on the cross sections for pion absorption by  $T=0$  and  $T=1$  nucleon pairs. They found surprisingly large ratios for  $d\sigma(\pi^+, pp)/d\sigma(\pi^-, pn)$ , on the order of  $\sim 100$ . By counting the numbers of initial nucleon pairs with the isospin  $T=0$  and  $T=1$  in those nuclei, these ratios were expressed in terms of the isospin of initial nucleon pairs. It was then found that  $R \equiv d\sigma(T=0)/d\sigma(T=1) \sim 50$ .<sup>1</sup> If one estimates this ratio in terms of the isospin geometry for the formation of  $\Delta$  isobars, one finds  $R = 2$ .<sup>1,2</sup>

In this short note, we would like to demonstrate that our current understanding of the pion nucleon interaction and the  $\Delta$  isobar formation provides a natural explanation for the observed large value of this ratio.

In recent years, there have been a number of theoretical derivations of the pion-nucleus optical potential parameters from the pion-nuclear many body theory.<sup>3-11</sup> In particular, the imaginary part of the two body optical potential has a direct relationship to pion absorption. The S-wave and P-wave pion absorption mechanisms seem to provide a microscopic understanding of the optical parameters derived from pionic atoms and pion-nucleus elastic scattering cross sections.<sup>12</sup> The S-wave pion absorption mechanism accounts for the experimental fall off of the  $\pi d \rightarrow pp$  cross section with increasing pion energy and becomes negligibly small above  $T_\pi \approx 50$  MeV. On the other hand, the P-wave pion absorption mechanism,

in particular through the  $\Delta$  isobar intermediate excitation, becomes dominant above  $T_\pi \approx 100$  MeV.

Since our interest is in pion absorption in the resonance energy region, we concentrate on the P-wave absorption process through the  $\Delta$  isobar intermediate excitation alone, as depicted in Fig. 1. The wavy lines denote the spin isospin dependent interaction which is usually described in terms of the pion and rho meson exchanges.<sup>14</sup> The T-matrix for pion absorption by the pion exchange mechanism is obtained by the Feynman graph technique in momentum space;

$$\begin{aligned}
T(\vec{k}_1, \vec{k}_2; \vec{k}) &= \frac{f(k_1)}{\mu} (\vec{\sigma}_1 \cdot \vec{k}_1) \vec{\tau}_1 \cdot D_\pi(\vec{k}_1) \frac{f^*(k_1)}{\mu} (\vec{S}_2^+ \cdot \vec{k}_1) \cdot \vec{T}_2^+ G_D(\vec{P}_\Delta) \frac{f(k)}{\mu} \vec{S}_2 \cdot \vec{k} \vec{T}_{2\lambda} \\
&+ \frac{f(k_1)}{\mu} (\vec{\sigma}_1 \cdot \vec{k}_1) \vec{\tau}_1 \cdot D_\pi(\vec{k}_1) \frac{f^*(k_1)}{\mu} (\vec{S}_2 \cdot \vec{k}_1) \cdot \vec{T}_2 G_C(\vec{P}_\Delta) \frac{f(k)}{\mu} \vec{S}_2^+ \cdot \vec{k} \vec{T}_{2\lambda} \\
&+ (1 \leftrightarrow 2).
\end{aligned} \tag{1}$$

Here  $\vec{k}$  is the incoming pion momentum in the laboratory frame, which after absorption gets distributed as  $\vec{k}_1$  and  $\vec{k}_2$  among the two nucleons 1 and 2 involved in the process.  $\vec{\sigma}, \vec{\tau}$  are the spin, isospin Pauli matrices and  $\vec{S}, \vec{T}$  the corresponding transition operators between a nucleon and a  $\Delta$  isobar. The  $\pi N\Delta$  coupling constant  $f^*$  is related to the  $\pi NN$  coupling constant  $f$  through  $f^* = 2f$  (Chew-Low relation) and has the monopole form factor  $f^*(k) = \left( \frac{\Lambda^2 - \mu^2}{\Lambda^2 - k^2} \right) f^*$ , where  $\Lambda$  is the cutoff mass.  $D_\pi$  is the pion propagator and  $\mu$  the pion mass. The  $\Delta$  isobar propagators for the direct (Fig. 1(a) and (c)) and the

crossed (Fig. 1(b) and (d)) graphs are

$$\begin{aligned} G_D(\vec{P}_\Delta)^{-1} &= m_\Delta - m + \vec{P}_\Delta^2/2m_\Delta - \omega - \frac{1}{2} i\Gamma \\ G_C(\vec{P}_\Delta)^{-1} &= m_\Delta - m + \vec{P}_\Delta^2/2m_\Delta + \omega, \end{aligned} \quad (2)$$

where the  $\Delta$  isobar mass and nucleon mass are denoted by  $m_\Delta$  and  $m$  and the pion energy by  $\omega$ . We take the static nucleon approximation and therefore  $|\vec{P}_\Delta|^2 = |\vec{k}|^2$  for  $G_\Delta$  and  $|\vec{P}_\Delta|^2 = m\omega$  for  $G_C$ . For the width of the  $\Delta$  isobar, we take the empirical relation.<sup>15</sup>

$$\Gamma = \frac{0.47}{1 + 0.6(q/\mu)^2} \frac{q^3}{\mu^2}. \quad (3)$$

The pion-nucleon center-of-mass momentum  $q$  is related to the incoming pion momentum through  $\vec{q} = \frac{m}{\sqrt{s}} \vec{k}$ , where  $s$  is the s-channel invariant mass.

The T-matrix (Eq. 1) together with a similar expression for the rho meson exchange process can be further worked out using the technique developed in Ref. 6. A lengthy expression is then obtained for pion absorption in terms of two body transition operators in the nucleon space, the details of which will be published elsewhere.<sup>16</sup>

In principle, many pion partial waves contribute to the absorption cross section;  $\ell_\pi$  (pion partial wave)  $\lesssim k \cdot R$  (nuclear radius). However, for the sake of discussion let us take the dominant partial wave  $\ell_\pi = 1$ , absorption of which by a 1S-orbit nucleon leaves the intermediate  $\Delta$  isobar in the 1S-orbit.<sup>1</sup> In this case, the ratio  $R$  does not depend on any details of the model parameters and is simply given by the ratio of the squares of the  $\Delta$  isobar propagators  $G_D$  and  $G_C$  of Eq. (2);

$$R = \frac{d\sigma(T=0)}{d\sigma(T=1)} = \left| \frac{G_D}{G_C} \right|^2 \quad (4)$$

The calculated ratio using Eq. (4) is shown by the dashed line in Fig. 2. Because of the resonant behavior in the direct channel, the ratio has a peak at  $k \sim 2\mu$  ( $T_\pi \sim 180$  MeV). At the experimental energy,  $T_\pi = 165$  MeV,<sup>1</sup> this ratio is  $\sim 200$ . This behavior is understood as follows. While  $\ell_\pi = 1$  pion absorption by a  $T=0$  nucleon pair is allowed by the direct absorption mechanism (Fig. 1(a) and (c)), this is forbidden for a  $T=1$  nucleon pair. For the latter case, absorption of a  $\ell_\pi = 1$  pion by a  $T=1$  pair ( $S=0, L=0$ ) leads to  $T=1, J^\pi = 1^+$  intermediate states. Those quantum numbers are not allowed by the Pauli principle for the final nucleon pair. Instead, pion absorption by a  $T=1$  pair proceeds through the crossed absorption mechanism (Fig. 1(b) and (d)) with exactly the same matrix elements as the direct  $T=0$  absorption process except the  $\Delta$  isobar propagators.

A question to examine now is if other partial wave contributions in particular for  $T=1$  pion absorption are small enough to keep the ratio sufficiently large. One thing to note in this respect is that absorption of  $\ell_\pi \neq 1$  forces the intermediate  $\Delta$  isobar to move with a finite angular momentum ( $\ell_\Delta \neq 0$ ). This fact, together with the large momentum transfer ( $\Delta q \sim \sqrt{m\omega}$ ) between the two nucleons required for pion absorption<sup>13</sup> (short range process) tends to cut down to a great extent the spatial transition matrix between the initial and final states.

In the pion absorption operator, there is spin-spin interaction as well as the tensor interaction.<sup>6</sup> The large momentum transfer

requirement forces two nucleons to be in the short distance ( $r \lesssim 0.5$  fm), whereas the strong short range correlations prevent them from coming together. This interplay makes the contribution of the spin-spin interaction negligibly small.<sup>13</sup> Therefore, we shall take only the tensor interaction terms in our calculation. Furthermore, the ratio  $R$  weakly depends on the angle between the outgoing nucleons and we choose the angle such that the relative momentum of the nucleon pair is perpendicular to the incoming pion momentum. The results with pion exchange alone with a cutoff mass of  $\Lambda_\pi = 0.8$  GeV are shown in Table I. When this value of  $\Lambda_\pi$  is used in the  $\pi$  exchange model, it gives results similar to those of the standard  $(\pi + \rho)$  exchange model, where a larger value of  $\Lambda_\pi$  is used.<sup>13</sup> The results on the ratio are not very sensitive to the choice of  $\Lambda_\pi$  within the reasonable range.

We show in Table I the pion absorption cross sections in several channels for  $\ell_\pi \leq 2$  as a function of pion momentum  $k$ . The  $\ell_\pi = 0$  and 2 contributions are indeed very small as compared to the dominant one ( $\ell_\pi = 1, T = 0 \rightarrow T' = 1$ ) even up to large momenta considered here particularly for the initial isospin  $T = 1$  case. This is due to the small spatial matrix elements for  $\ell_\pi = 0$  and 2 as compared to those for  $\ell_\pi = 1$ , typically about 1/5 in the resonance region, and strong cancellation between the two competing terms for  $T = 1$ . Note that the explicit distinction between the direct and crossed  $\Delta$  propagators  $G_D$  and  $G_C$ , which was neglected by Ko and Riska,<sup>6</sup> is important for this cancellation. The higher partial wave contributions ( $\ell_\pi \geq 3$ ) are smaller by an order of magnitude.

The summed values for the  $T=0$  and  $T=1$  initial pairs are then used to derive the ratio  $R$  as a function of the pion momentum, which is depicted by the solid line in Fig. 2. The ratio is now down to about 40 at  $T_\pi = 165$  MeV. The experimental results taken at different angles are also shown with error bars.<sup>1</sup>

Finally as stated at the beginning, the S-wave pion absorption process ( $\ell_\pi = 0$ ) is important at low pion energies. Therefore, the calculated results have to be used with caution below  $T_\pi \approx 100$  MeV. The capture of pions from the 2p level in pionic atoms<sup>17</sup> might, however, be compared with the present result at  $T_\pi = 0$  MeV.<sup>6,10</sup> Furthermore, we have been neglecting the P-wave absorption process through nucleon intermediate states. This is certainly small for  $T=0$  pion absorption,<sup>13</sup> but might give an additional contribution for absorption by a  $T=1$  pair.

In conclusion, we have demonstrated that our knowledge of the pion nucleon interaction and the  $\Delta$  isobar formation gives a natural explanation for the large ratio of the pion absorption cross sections by  $T=0$  and  $T=1$  nucleon pairs in the resonance region. The resulting ratio  $R = \frac{d\sigma(T=0)}{d\sigma(T=1)}$  shows only a slight resonance behavior. It would be interesting to measure this energy dependence and also the angular distributions for a  $T=1$  pair, which should show an interesting variation with energy due to the interplay between the three ( $\ell_\pi = 0 \sim 2$ ) partial waves.

#### Acknowledgments

We are extremely grateful to G.F. Bertsch for introducing us to these interesting experimental data and for enlightening

discussions in the course of the work. Thanks are also due to G.E. Brown and W. Weise for stimulating discussions and to D. Ashery, E. Piassetzhy and J.P. Schiffer for experimental information. This work was supported by the National Science Foundation under grant no. PHY-80-17605.



References

1. D. Ashery, et al., Phys. Rev. Letters 47 (1981) 895.
2. J.N. Ginocchio, Phys. Rev. C17 (1978) 195;  
H.E. Jackson, et al., Phys. Rev. Lett. 39 (1977) 1601; H.E. Jackson, et al., Phys. Rev. C16 (1977) 730; R.D. McKeown, et al., Phys. Rev. Lett. 44 (1980) 1033; R.D. McKeown, et al., Phys. Rev. C24 (1981) 211.
3. F. Hachenberg and H.J. Pirner, Ann. of Phys. 112 (1978) 401.
4. G.F. Bertsch and D.O. Riska, Phys. Rev. C18 (1978) 317.
5. J. Chai and D.O. Riska, Nucl. Phys. A329 (1979) 429.
6. C.M. Ko and D.O. Riska, Nucl. Phys. A312 (1978) 217.
7. G.A. Miller, Phys. Rev. C16 (1977) 2335.
8. E. Oset, W. Weise and R. Brockmann, Phys. Lett. 82B (1979) 344.
9. R. Rockmore, E. Kanter and P. Goode, Phys. Lett. 77B (1978) 149.
10. K. Shimizu and A. Faessler, Nucl. Phys. A306 (1978) 311.
11. D.O. Riska and H. Sarafian, Phys. Rev. C22 (1980) 1222.
12. K. Stricker, H. McManus and J. Carr, Phys. Rev. C19 (1979) 929.
13. O.V. Maxwell, W. Weise and M. Brack, Nucl. Phys. A348 (1980) 388 and references therein.
14. E. Oset, H. Toki and W. Weise, Phys. Rep. 83 (1982) 281.
15. A. Rittenberg et al., (Particle Data Group), Rev. Mod. Phys. 43 (1971) S114.
16. H. Toki and H. Sarafian, to be published.
17. M.E. Nordberg, K.E. Kinsey and R.L. Burman, Phys. Rev. 165 (1968) 1096.

Table I. Pion absorption cross sections in several channels as a function of pion momentum  $k$  are compared, where  $\ell_\pi$  is the angular momentum of the incoming pion. These numbers are normalized to the  $(T,S,L) = (0,1,0)$  to  $(T',S',L') = (1,0,2)$  transition at  $k=0.5\mu$  as indicated by \*.

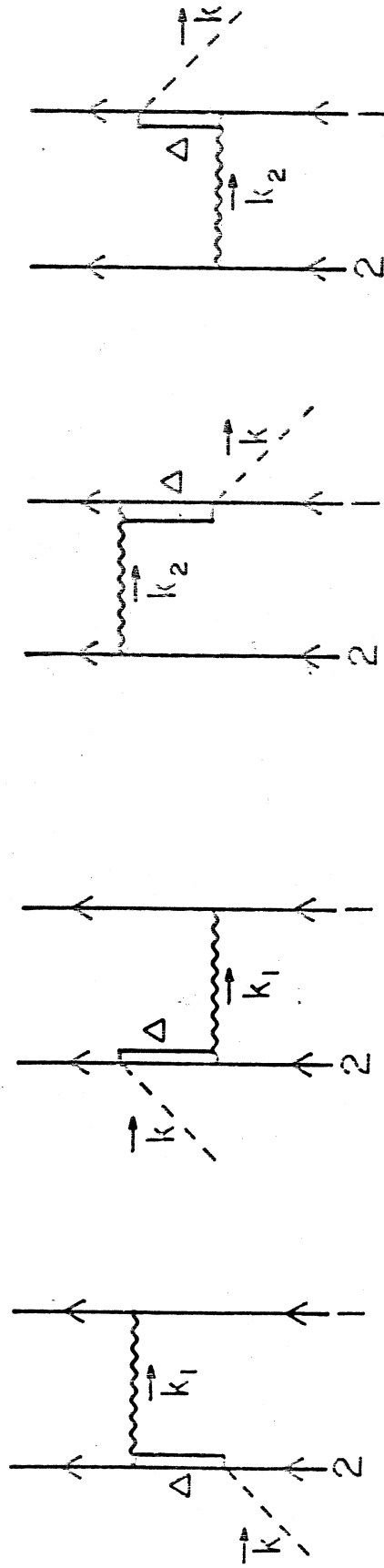
$k[\mu]$					0.5	1.0	1.5	2.0	2.5
Initial	$\ell_\pi$	T'	S'	L'					
T=0	0	1	1	1	0.027	0.40	2.9	9.7	7.3
S=1	1	1	0	2	1*	4.9	21	52	30
L=0	2	1	1	3	0.006	0.11	1.0	4.2	3.6
T=1	0	1	1	1	0.008	0.086	0.44	1.1	0.63
S=0	1	0	1	2	0.076	0.17	0.24	0.26	0.26
L=0	2	1	1	3	0.002	0.023	0.14	0.40	0.26

Figure Captions

Fig. 1 - P-wave pion absorption mechanism with  $\Delta$  isobar intermediate excitation

Fig. 2 - The pion absorption ratio  $R = \frac{d\sigma(T=0)}{d\sigma(T=1)}$  as a function of the pion momentum  $k$  ( $T_\pi = \text{kinetic energy}$ ). The dashed line denotes the  $\ell_\pi = 1$  contribution only (Eq. 4), whereas the solid line includes all. The experimental data taken at different angles at  $T_\pi = 165$  MeV are depicted by the points with error bars.

MSUX-82-178



(a)

(b)

(c)

(d)

FIGURE 1

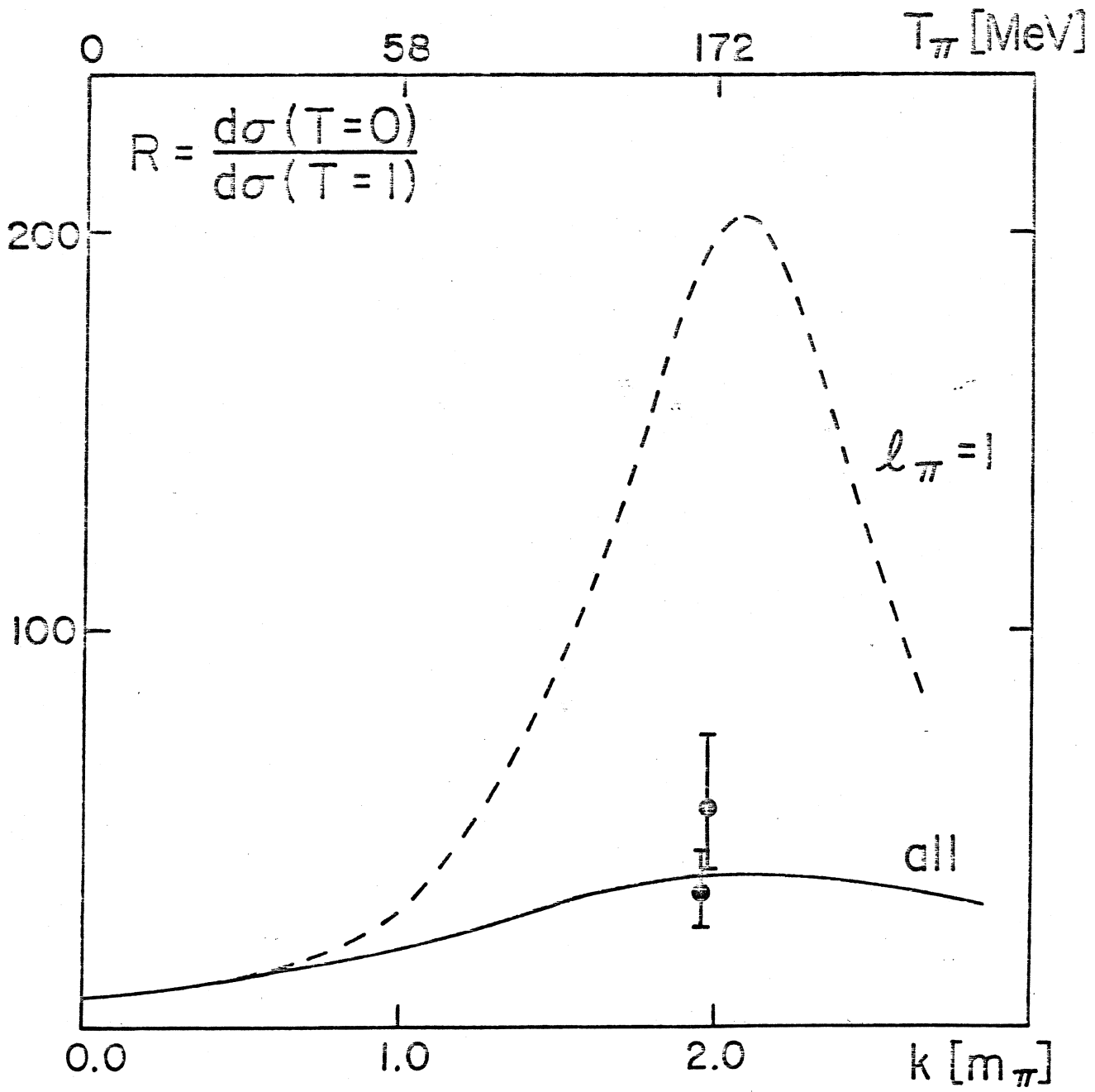


FIGURE 2